The low-energy absorption and reflectivity of $Hg_2P_2S_6$ and $Hg_2P_2Se_6$

1997 J. Phys.: Condens. Matter 9 4791

(http://iopscience.iop.org/0953-8984/9/22/029)

J. Phys.: Condens. Matter **9** (1997) 4791–4799. Printed in the UK PII: S0953-8984(97)80658-3

The low-energy absorption and reflectivity of $Hg_2P_2S_6$ and $Hg_2P_2Se_6$

C Calareso, V Grasso, F Neri and L Silipigni

Dipartimento di Fisica della Materia e Tecnologie Fisiche Avanzate, Università di Messina, and Istituto Nazionale per la Fisica della Materia, Unità di Messina, Salita Sperone 31, I-98166, Messina, Italy

Received 6 January 1997, in final form 25 February 1997

Abstract. Absorption and reflectivity measurements have been performed on $Hg_2P_2S_6$ and $Hg_2P_2Se_6$ samples in the energy range from 1.6 to 5.5 eV at room temperature. Optical absorption results indicate that the absorption edge arises from a direct transition for both compounds. The reflectivity spectra show a striking similarity: two maxima are present in both materials for photon energies greater than that of the absorption edge. These structures have been interpreted as direct allowed interband transitions. The interpretation is based on the so-called transition metal weakly interacting model. In order to indicate the possible electronic transitions responsible for the observed reflectivity structures, a schematic energy level diagram is proposed for both compounds.

1. Introduction

In the past few decades, much work, both experimental and theoretical, has been devoted to the determination of the electronic energy band structure of the $M_2P_2X_6$ compounds, where M is a transition metal or post-transition metal, and X stands for S or Se. In particular, attention has been focused on those members of the family showing a number of interesting chemical and physical properties, e.g. the intercalation of lithium in the layered compound $Ni_2P_2S_6$ [1], the antiferromagnetic ordering in, e.g., $Mn_2P_2S_6$ or $Mn_2P_2Se_6$ [2], the photoelectrochemical response of $Fe_2P_2S_6$, $Ni_2P_2S_6$, and $Sn_2P_2S_6$ [3], or the ferroelectric properties of $Sn_2P_2S_6$ [4].

Recently, the possibility of bestowing specific properties on some transition metal chalcogenophosphates through the intercalation of specifically functionalized molecules, such as cationic chromophores chosen for their hyperpolarizability (4′-dimethylamino-*N*-methylstilbazolium: $DAMS^+$ [5]), or fundamental molecules in the field of organic conductors (tetrathiafulvalene [6]), has opened up a new avenue of research in the field of 'multiproperty' materials [7], increasing the interest in this family of compounds. In this context, it seems reasonable to investigate the less-examined $M_2P_2X_6$ compounds—in particular the mercury phases—in order to discover their physical properties, and consequently their possible technological applications.

For the mercury compounds, only a crystal structure analysis, as far as we are aware, has been reported in the literature. According to this structural investigation [8], $Hg_2P_2S_6$ crystallizes in a triclinic structure and $Hg_2P_2Se_6$ in a monoclinic one. Notwithstanding this symmetry difference, both structures are characterized by P_2S_6 and P_2Se_6 groups which are connected by the Hg atoms to form analogous layers situated parallel to the *ab*-plane. The

0953-8984/97/224791+09$19.50

main difference from the crystal structure of the other $M_2P_2X_6$ compounds of $Fe_2P_2X_6$-type lies in the coordination of the metal by the chalcogen atoms. In fact, while the transition metals of the first series are coordinated octahedrally by the sulphur or selenium atoms, for the mercury atoms an approximately tetrahedral coordination results in agreement with the tendency of the mercury ion to form lower-coordination bonds in various compounds [8]. In spite of this metal coordination difference, the symmetry of the $(P_2S_6)^{4-}$ and $(P_2Se_6)^{4-}$ clusters can be described by the space group D_{3d} as in the case of the $Ni_2P_2S_6$ compound [9], showing therefore a close relationship of the $Hg_2P_2X_6$ structures to the $Fe_2P_2X_6$-type ones. In the light of these observations it is important to obtain information about the chemical and physical properties of $Hg_2P_2X_6$, and in particular about their electronic structure, before a complete energy band model of the $M_2P_2X_6$ compounds can be worked out.

In this paper we present a study of some optical properties of the $Hg_2P_2S_6$ and $Hg_2P_2Se_6$ compounds, based on room temperature absorption and reflectivity measurements for the photon energy range from 1.6 to 5.5 eV. The effect on a given spectrum of replacing S by Se has also been examined.

2. Experimental details

The samples of $Hg_2P_2S_6$ and $Hg_2P_2Se_6$ used in this work were grown and supplied by LPME of the Institut de Physique Appliquée of the École Polytechnique Fédérale de Lausanne. While the $Hg_2P_2S_6$ crystals appear as transparent gold–yellow plates, the $Hg_2P_2Se_6$ ones are silver–red plates. The colours of the compounds appear to be governed, as already observed for other chalcogenophosphates [10], by the rule that the replacement of S by Se shifts the absorption edges towards longer wavelengths. All of the spectra were obtained at room temperature, between 1.6 and 5.5 eV, with unpolarized light at normal incidence on the crystal surface, using a Perkin–Elmer double-beam UV–visible spectrophotometer, model Lambda 2. For the reflectivity measurements a specular accessory was used. The sample thickness ranged between 50 μm and 300 μm for $Hg_2P_2S_6$ and between 15 μm and 100 μm for $Hg_2P_2Se_6$. All of the measurements were repeated several times to check for their reproducibility.

3. Results

Figures 1(a) and 1(b) show the room temperature reflectivity spectra measured in the energy range from 1.6 to 5.5 eV for $Hg_2P_2S_6$ and $Hg_2P_2Se_6$ respectively. A pronounced rise in the reflectivity spectral response near the fundamental absorption edges was observed for both compounds. Similar reflectivity increases are common to most of the layer-type materials [11]. Following Elkorashy [11], we have calculated, in the absence of interference, the true reflectivity R_s, i.e. the fraction of incident radiation that is reflected from the first surface, by simultaneously solving the following equations:

$$R = R_s\left[1 + \frac{(1-R_s)^2\exp(-2\alpha d)}{1-R_s^2\exp(-2\alpha d)}\right] \tag{1}$$

$$T = \frac{(1-R_s)^2\exp(-\alpha d)}{1-R_s^2\exp(-2\alpha d)} \tag{2}$$

where R and T are the measured sample reflectivity and transmissivity at normal incidence respectively, α is the absorption coefficient, and d is the thickness of the sample. In figures

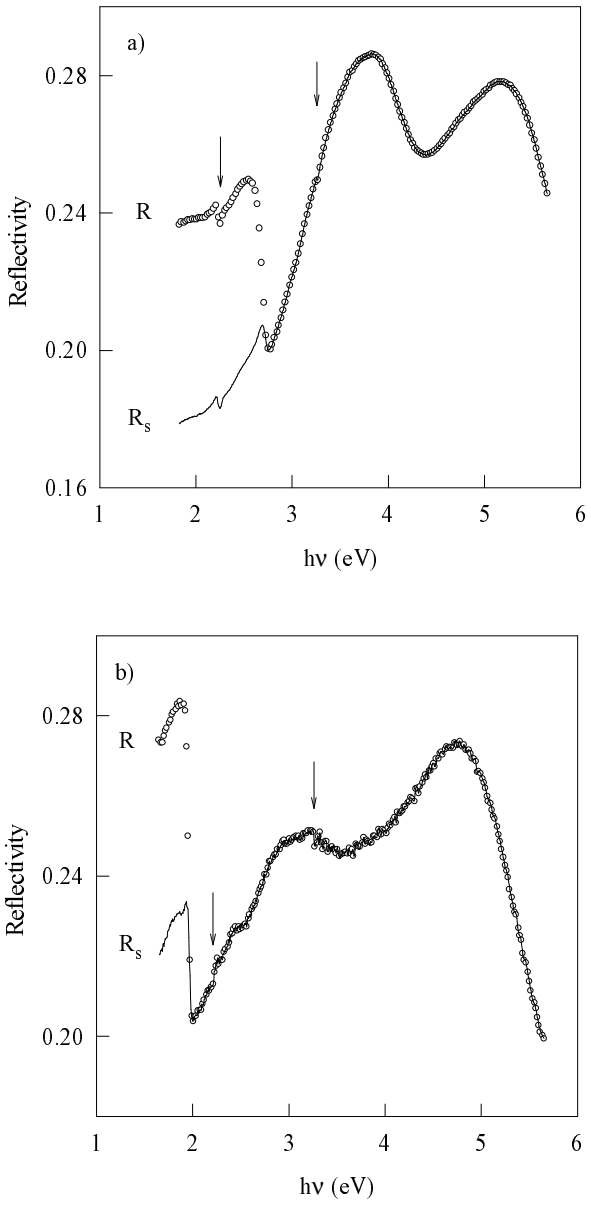

Figure 1. The room temperature reflectivity spectral response of $Hg_2P_2S_6$ (a) and $Hg_2P_2Se_6$ (b). The open circles represent the experimental R-data; the solid line is the one-surface reflectivity R_s calculated by simultaneous solution of equations (1) and (2). The arrows indicate two structures due to instrumental factors.

1(a), 1(b), the open circles represent the measured sample reflectivity R, while the solid line represents the one-surface reflectivity R_s.

Inspection of figures 1(a), 1(b) reveals that for photon energies greater than the absorption edge the gross features are broadly similar for the two compounds: between 2.7 eV and 5.5 eV for $Hg_2P_2S_6$ and between 2.0 eV and 5.5 eV for $Hg_2P_2Se_6$, two broad

peaks occur with shoulders more or less evident on their low-energy side. Two structures between 2.1 and 2.3 eV and between 3.2 and 3.3 eV, indicated with arrows in figures 1, are present in all of the spectra, and are due to instrumental factors.

Figures 2(a), 2(b) show the behaviour of the total absorption coefficient α as a function of the photon energy, $h\nu$, around the absorption edge for a $Hg_2P_2S_6$ sample with a thickness of 268 μm, and for a $Hg_2P_2Se_6$ specimen with a thickness of 18 μm, respectively. This quantity was directly calculated from the absorbance and reflectivity data for $Hg_2P_2S_6$ and $Hg_2P_2Se_6$, respectively, by using the following expression:

$$\alpha = \frac{1}{d} \ln \left(B + \sqrt{B^2 + R_s^2} \right) \tag{3}$$

deduced by solving equation (2) for α. In equation (3), d is the sample thickness and $B = (1 - R_s)^2/2T$. For both compounds, α did not reach zero for any value of the photon energy, but shows a featureless long tail on the low-energy side, which is, as will be discussed in the following section, a feature common to most layer-type crystals. From an analogy with certain layered compounds [11], we have assumed that the total absorption coefficient α consists of two terms; that is,

$$\alpha = \alpha_0 + \alpha_i . \tag{4}$$

In equation (4), α_i is the interband absorption coefficient, which predominates for photon energies sufficiently higher than the fundamental absorption edge, while α_0, which dominates below the fundamental absorption edge, is the absorption coefficient due to other mechanisms, as will be discussed later on. In order to obtain the interband absorption coefficient α_i, we extrapolated the low-energy part of the absorption coefficient, and subtracted it from the total absorption coefficient α. The extrapolation of α_0 is shown in figures 2(a), 2(b) with dashed lines.

Further information can be obtained from figures 3(a), 3(b), where $(\alpha_i E)^{2/3}$ is plotted against the incident photon energy, $h\nu$, for $Hg_2P_2S_6$ and $Hg_2P_2Se_6$, respectively. The linear region of these curves indicates the existence of a forbidden direct band gap, whose values of 2.67 eV for $Hg_2P_2S_6$ and of 1.95 eV for $Hg_2P_2Se_6$ have been determined by extrapolating the linear branch of the curve down to zero.

4. Discussion

Before discussing the reflectivity spectra of $Hg_2P_2S_6$ and $Hg_2P_2Se_6$, we recall that in these compounds, as in several transition metal compounds [12], four main kinds of transition may occur:

(i) the *d–d* transitions;

(ii) the *charge-transfer* transitions from the valence bands to the levels localized on the metal ion;

(iii) the *orbital promotion* transitions from the localized transition metal d states to the empty conduction band states; and

(iv) the *interband* transitions between the valence and the conduction bands.

For the compounds investigated we cannot observe d–d transitions or charge-transfer transitions from the valence bands to the Hg 5d levels, since these latter are completely full.

As regards the *charge-transfer* transitions from the valence bands to the Hg 6s states, it can be assumed, as will be discussed in the following, in analogy to other $M_2P_2S_6$ compounds [9, 13], that in $Hg_2P_2S_6$ and $Hg_2P_2Se_6$ the metal s states constitute the highest

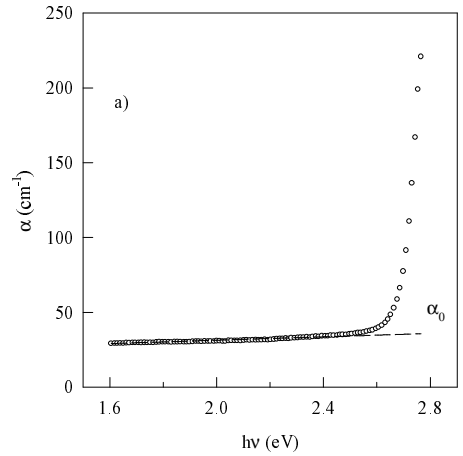

Figure 2. The spectral response of the total absorption coefficient α of $Hg_2P_2S_6$ (a) and $Hg_2P_2Se_6$ (b) in the region of the fundamental absorption edge. This quantity was directly calculated from the measurements of absorbance and reflectivity according to equation (3) for samples with thicknesses of 268 μm and 18 μm, respectively. The dashed lines represent the extrapolation of the low-energy tail α_0.

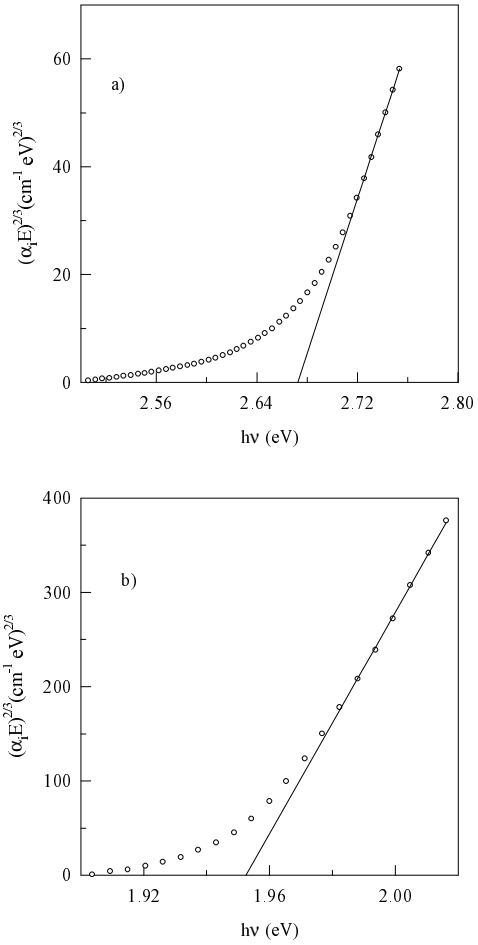

Figure 3. A plot of $(\alpha_i E)^{2/3}$ versus the incident photon energy, $h\nu$, near the absorption edge, for $Hg_2P_2S_6$ (a) and $Hg_2P_2Se_6$ (b). The solid lines represent the extrapolation of the linear branch of the curve down to zero.

conduction bands. In this hypothesis, the above-mentioned transitions will take place in the far-ultraviolet region, and therefore they do not contribute to the observed reflectivity structures.

For the *orbital promotion* transitions, according to our preliminary photoemission measurements [14], in $Hg_2P_2S_6$ and $Hg_2P_2Se_6$ the filled Hg 5d states lie at least 9 eV below the Fermi level. Consequently the transitions from the Hg 5d levels play no role in the reflectivity spectra below 9 eV.

Therefore, the observed reflectivity features can only be attributed to *interband* transitions. Since no band-structure calculation exists for these chalcogenophosphates of mercury, it is tempting to identify the states involved in these transitions by analogy with

some $M_2P_2S_6$ compounds, in particular with $Ni_2P_2S_6$ and $Zn_2P_2S_6$. For these compounds, Piacentini *et al* [9, 15] proposed a semi-empirical energy level scheme based on the single-layer approximation and on an ionic model, the so-called transition metal weakly interacting model, in which the cluster $(P_2S_6)^{4-}$ and the M^{2+} ion are treated separately. In this scheme, for the cluster $(P_2S_6)^{4-}$, the energy levels of the symmetrized combination of the phosphorus 3s, 3p and the sulphur 3s, 3p states are obtained empirically from the comparison with the valence band x-ray photoemission spectra, while, for the M^{2+} ion, its d orbitals, viewed as discrete and localized, are located within the (P–P) p bonding–antibonding gap if they are partially empty, or below the main valence band if they are completely full. Thus, the highest valence bands are formed by the (P–P) p bonding states and S 3p nonbonding levels, while the lowest conduction bands are constituted mostly by the (P–P) p antibonding and the S p bonding and antibonding states. According to this scheme, which assigns no role in the bonding to the M^{2+} d states, all of the $M_2P_2S_6$ compounds should have similar optical and XPS spectra, except those structures directly involving transitions to or from the metal d levels. Thus, in the authors' opinion [9], this scheme should also be valid for other compounds similar to $Ni_2P_2S_6$, i.e. those with other metals in place of Ni, and those with Se in place of S.

In the light of these observations, and since in the mercury chalcogenophosphates investigated, as reported in the literature [8], the symmetry of the cluster $(P_2X_6)^{4-}$ can be described by the D_{3d} space group, as in the case of $Ni_2P_2S_6$ [9], we use the energy level scheme of Piacentini *et al* as a basis for interpreting the observed reflectivity structures. Hypothesizing, in analogy to the case for $Ni_2P_2S_6$, that in $Hg_2P_2S_6$ and $Hg_2P_2Se_6$, mercury probably occurs as a bivalent ion, i.e. Hg has lost its $6s^2$ electrons, and its 5d states are discrete and localized below the main valence band as in the case of $Zn_2P_2S_6$ [15], we draw a possible schematic energy level diagram for $Hg_2P_2S_6$ and $Hg_2P_2Se_6$ as shown in figures 4(a) and 4(b), respectively. In these figures the interband transitions that lead to the reflectivity structures are also indicated with arrows. The highest valence bands are formed by the (P–P) p bonding states and X 3p nonbonding levels, while the lowest conduction bands are constituted mostly by the (P–P) p antibonding states and by the X p bonding and antibonding states. Then the two groups of structures observed in the reflectivity data, each one constituted by a peak with a shoulder on the low-energy side, and located between 2.7 eV and 5.5 eV in $Hg_2P_2S_6$ and between 2.0 eV and 5.5 eV in $Hg_2P_2Se_6$, arise from the excitation of the p electrons of the P and S atoms, i.e. as transitions between bands based on these levels. In particular, assuming that in $Hg_2P_2S_6$, in analogy to the case for $Ni_2P_2S_6$, the (P–P) p bonding states are located at 2.3 eV above the S 3p nonbonding states [9], the first group of structures, positioned at around 3.8 eV, can be attributed to the electronic transitions from the (P–P) p bonding band to the S p bonding and antibonding states (transitions I in figure 4(a)), while the second group, located at around 5.0 eV, can be attributed to the electronic transition from the S p nonbonding states to the (P–P) p antibonding states (transition II in figure 4(a)). For $Hg_2P_2Se_6$, it is possible to assign the two groups of structures, located at around 3.0 eV and 4.5 eV, to the same electronic transitions, as can be seen in figure 4(b) (transitions I and II), even if these features are positioned at lower energies. In fact, as will be discussed later, this shift is due to replacing S by Se.

The pronounced rise near the absorption edge can be explained as being partially due to the back-surface reflection, resulting in multiple reflections within the sample [11, 16–18]. From figures 1, it is seen that the correction for the back reflection reduces the rise in reflectivity for both compounds, but does not remove it completely. In fact, the one-surface reflectivity R_s still exhibits a small increase. This residual increase can be the result of

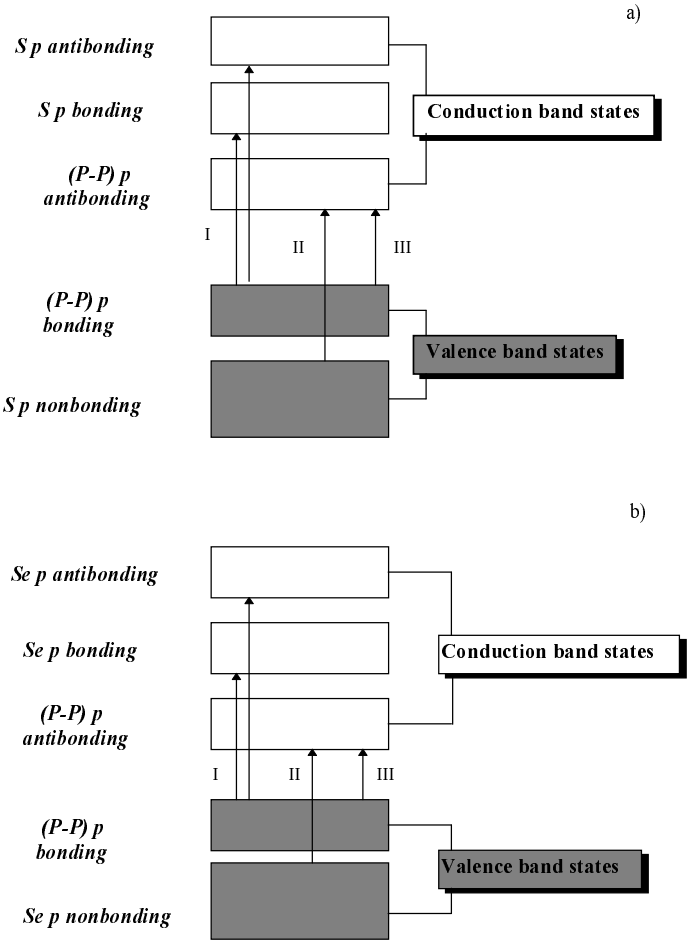

Figure 4. Schematic energy level diagrams for $Hg_2P_2S_6$ (a) and $Hg_2P_2Se_6$ (b), derived from the simplified energy level scheme formulated by Piacentini *et al* for other $M_2P_2S_6$ compounds. The arrows indicate the electronic transitions responsible for the observed reflectivity structures (transitions I and II) and for the absorption edge (transition III).

either or both of two concomitant causes. The first one is, in agreement with the literature [11], the scattering caused by the cleavage planes within the sample which are parallel to its surfaces. The second possible cause is the presence of a structure associated with the absorption edge. In fact, an absorption edge, such as an allowed direct interband transition, should manifest itself as a peak in reflectivity [19].

From the results of the absorption measurements, we can assert that for both compounds, in addition to the interband fundamental absorption, at least one mechanism of absorption exists. Similar results were reported in the literature for crystals with layer-type character, such as GeS, SnSe, SnS, SnS_2, and $SnSe_2$ [16–18], where a low-energy tail in the absorption spectrum was observed and attributed to internal photon scattering by the layer structure of the materials investigated. On the basis of the present results alone, we hypothesize an analogous nature for α_0. The fact that α_0 seems to be more or less constant or proportional to λ^{-1}, as can be seen from figures 2, seems to favour this hypothesis, thus excluding the

possibility of an absorption due to free carriers or excitons. In fact, an absorption due to free carriers should give a λ^2-dependence for α_0, while an absorption due to excitons should extend over a small range of photon energies below the fundamental edge [16].

Neglecting the exciton formation, we have examined the form of the interband absorption coefficient α_i as a function of photon energy, $h\nu$, near the absorption edge, in order to obtain information about the type of transition at the absorption edge. Plotting $(\alpha_i E)^{2/3}$ against E, a linear region is observed, the existence of which indicates that the interband absorption near the absorption edge is caused by forbidden direct transitions. The presence near the absorption edge of the residual increase in reflectivity, also perhaps caused by a structure associated with the absorption edge, would favour a direct allowed transition, but the small values obtained for the absorption coefficient and the above-mentioned behaviour seem to be more in agreement with an electric-dipole-forbidden transition that becomes allowed in a higher degree of approximation (magnetic dipole or spin–orbit interaction effects). Therefore, we come to the conclusion that the direct forbidden transition is the most probable type of transition near the fundamental absorption edge. On the basis of the schematic diagram, derived from the simplified energy level scheme proposed by Piacentini *et al* [9] and represented in figures 4, we attribute the optical energy gap, obtained by extrapolating the linear branch of the curve $(\alpha_i E)^{2/3}$ versus E down to zero, to the dipole-forbidden transition from the bonding (P–P) p band to the antibonding (P–P) p one, which, as reported in the literature [15], becomes allowed due to the spin–orbit interaction.

As regards the effect of selenium, we note that Se in the place of S reduces, as expected, the (P–P) p bonding–antibonding gap arising in the valence band of the selenophosphate relative to that of the thiophosphate, as shown in figures 4 (transition III). The observed shift to lower energy of the observed reflectivity structures in going from $Hg_2P_2S_6$ to $Hg_2P_2Se_6$ can be attributed to the increased covalency on substituting Se for S [20].

5. Conclusion

Using the energy level scheme of Piacentini *et al* as a basis, we have proposed a schematic energy level diagram for $Hg_2P_2S_6$ and $Hg_2P_2Se_6$: all of the peaks observed in the reflectivity spectra have been accounted for as transitions between valence and conduction levels based on the P and S atoms. In particular, the first group of structures, positioned at around 3.8 eV in $Hg_2P_2S_6$ and around 3.0 eV in $Hg_2P_2Se_6$, have been attributed to the electronic transitions from the bonding (P–P) p band to the X p bonding and antibonding states, while the second group, at around 5.0 eV in $Hg_2P_2S_6$ and at around 4.5 eV in $Hg_2P_2Se_6$, have been attributed to the electronic transitions from the X p nonbonding states to the (P–P) p antibonding states.

These transitions shift to lower energies on going from $Hg_2P_2S_6$ to $Hg_2P_2Se_6$: this is the effect in the reflectivity spectra of substituting Se for S, and it can be attributed to an increased covalency due to this substitution.

From the absorption data, corrected for the reflectivity data, the result is obtained that these materials are broad-band semiconductors ($E_g = 2.67$ eV for $Hg_2P_2S_6$ and $E_g = 1.95$ eV for $Hg_2P_2Se_6$) in accord with other members of the $M_2P_2X_6$ compound family. For each case, the fundamental absorption edge has been assigned to the electronic transition between the (P–P) p bonding and antibonding states.

From the above results we come to the conclusion that the so-called transition metal weakly interacting model can be used satisfactorily to interpret the optical properties analysed for $Hg_2P_2S_6$ and $Hg_2P_2Se_6$ compounds in the energy range investigated.

Acknowledgments

We wish to thank H Berger and Professor G Margaritondo of the Institut de Physique Appliquée of the École Polytechnique Fédérale de Lausanne for supplying the crystals of $Hg_2P_2S_6$ and $Hg_2P_2Se_6$ that were investigated.

References

[1] Thompson A H and Whittingham M S 1977 *Mater. Res. Bull.* **11** 741
[2] LeFlem G, Brec R, Ouvrard G, Louisy A and Segrasan P 1982 *J. Phys. Chem. Solids* **43** 455
[3] Byvik C E, Smith B T and Reichman B 1982 *Solar Energy Mater.* **7** 213
[4] Carpentier C D and Nitsche R 1974 *Mater. Res. Bull.* **9** 1097
[5] Lacroix P G, Clément R, Nakatani K, Zyss J and Ledoux I 1994 *Science* **263** 658
[6] Lomas L, Lacroix P, Audiere J P and Clément R 1991 *J. Mater. Chem.* **1** 475
[7] Nicoud J F 1994 *Science* **263** 636
[8] Von Jandali M Z, Eulenberger G and Hahn H 1978 *Z. Anorg. Allg. Chem.* **447** 105
[9] Piacentini M, Khumalo F S, Olson G C, Anderegg J W and Lynch D W 1982 *Chem. Phys.* **65** 289
[10] Carpentier C D and Nitsche R 1974 *Mater. Res. Bull.* **9** 401
[11] Elkorashy A M 1988 *J. Phys. C: Solid State Phys.* **21** 2595
[12] Guizzetti G, Nosenzo L, Pollini I, Reguzzoni E, Samoggia G and Spinolo G 1976 *Phys. Rev.* B **14** 4622
[13] Khumalo F S and Hughes H P 1981 *Phys. Rev.* B **23** 5375
[14] Currò G M, Grasso V and Silipigni L 1996 internal report (Università di Messina)
[15] Piacentini M, Khumalo F S, Leveque G, Olson G C and Lynch D W 1982 *Chem. Phys.* **72** 61
[16] Elkorashy A M 1986 *Phys. Status Solidi* b **135** 707
[17] Elkorashy A M 1986 *J. Phys. Chem. Solids* **47** 497
[18] Domingo G, Itogaand R S and Kannewurf C R 1966 *Phys. Rev.* **143** 536
[19] Tauc J 1962 *Proc. Int. Conf. on the Physics of Semiconductors (Exeter, 1962)* (Bristol: Institute of Physics Publishing and the Physical Society) p 333
[20] Banda E J K B 1986 *Phys. Status Solidi* b **138** K125